JETIR.ORG ISSN: 2349-5162 | ESTD Year : 2014 | Monthly Issue

JOURNAL OF EMERGING TECHNOLOGIES AND INNOVATIVE RESEARCH (JETIR)

An International Scholarly Open Access, Peer-reviewed, Refereed Journal

ANALYSIS OF REFRIGERATION CYCLE EJECTOR

[1]POONAM PUROHIT
[1]ASSISTANT PROFESSOR

[2] MANISH KUVADIYA
[2] ASSISTANT PROFESSOR

[1]MECHANICAL ENGINEERING DEPARTMENT,
[1]PARUL UNIVERSITY, VADODARA, INDIA

Abstract: The use of ejector cycles for increased performance and efficiency is becoming more prevalent in industry. The goal of this study is to evaluate an ejector using Computational Fluid Dynamics (CFD) to evaluate flow patterns, perform trade studies varying the type of refrigerant, and determine the entrainment ratio for each working fluid, over a range of boundary condition pressures, set at points along the ejector's flow path. The 2012 Toyota Prius V is one of the first automobiles using an ejector cycle in their internal cabin refrigeration system. The DENSO Corporation ejector hardware was used as the basis for the creation of geometry for the CFD mode of the ejector. Three working fluids were simulated, R-134a, R-245fa, and R1234yf. The primary findings of this study were as follows. The CFD study here indicates that R-245fa performs the best out of the three working fluids, when examining their entrainment ratios (ratio of secondary to primary flow rates in the ejector). For all three working fluids, the entrainment ratio was seen to peak performance at an ejector inlet pressure of 1.75*105 Pa. The ejector mixing chamber pressure and ejector outlet pressure boundary conditions also witnessed a rise in entrainment ratios, during an increase of their respective pressure values.

Index Terms **– CFD, Ejector, Refrigeration, Simulation**

I. INTRODUCTION

With increasing regulation for carbon dioxide emission and environmental sustainability concerns, waste by product elimination, without decreasing performance, has become a primary goal for the future of automotive engineering. Much of the energy consumed by a conventional vehicle's air conditioning system can be attributed to the compressor, in the process of compressing refrigerant. Typical air conditioning systems use an expansion valve to relieve pressure from refrigerant, prior to passage through the evaporator to cool air. The DENSO Ejector system uses an ejector, instead of the expansion valve. The ejector accumulates energy previously lost through the expansion valve and stores it as pressure energy. The additional pressure increases efficiency and reduces power consumption..

II. LITERATURE REVIEW

The use of Computational Fluid Dynamics (CFD) is proliferate in the sector of ejector performance characterization. The work of [1] presents CFD results for an ejector using R-134a as the working fluid, and includes a comparison of the results based upon NIST REFPORPS interpolation of the fluids properties versus the ideal gas model. The investigation of [2] present the effects of temperature phase change on a two-phase ejector using CFD. The axial velocity, pressure, temperature, entrainment ratio, and volume fractions for gas and liquid two-phase LNG and boil off gas are presented. In the work of [3] a CFD study of an R-744 two phase ejector is presented. The CFD research of [4] gives a summary of ejector performance due to varying ejector primary nozzle geometry and surface roughness for an R-134a ejector. The CFD work of [5] presents simulations of a 2-D axisymmetric supersonic ejector using NIST real gas model integrated in ANSYS FLUENT for R-1234ze (E) and R-1234yf were used as working fluids. It is reported that using ideal gas model, the ejector entrainment ratio was overestimated up to 50.26% for R-1234yf and 25.66% for R-1234ze (E) higher than using real gas model. In the work of [6] ANSYS CFD is used with two solvers used for simulating R-32. The results of [6] showed that entrainment ratios were strongly influenced by the working conditions and that the pressure-based solver obtained comparable results with the density-based solver, while affording more stable solutions which converged faster than the density-based solver. In the research of [7] a CFD study of a two-stage ejector using the SST k-turbulence model shows that the entrainment ratios up to 77% are achievable using a two-stage ejector. In the work of [8] a comprehensive study of using CFD simulations to aid in the design of ejector is provided. There is it found that for a variety of different ejector geometries, the working fluid witness's transient phases in the ejector and subsequently, it is impossible to compress the vapors that eject from the refrigerant. The study of [9] CFD results are validated with available experimental data of R-134a converging-diverging nozzles in characterizing the flashing flow of R-134a in ejectors. From the study of [9] it is recommended that the optimum ratio of nozzle exit diameter to the throat diameter is D/d = 2.4. From the above literature review, we see that the use of

CFD to understand the behavior of ejectors used in refrigeration systems continues to be an on-going area of applied CFD research. To this end, the current paper presents a pragmatic based CFD study of the ejector used in a refrigeration system of a hybrid vehicle in order to help better understand the overall performance of the ejector within the context of the refrigeration cycle hardware in which it is being implemented. To the best of the author's collective knowledge the particular ejector configuration and working fluids studied herein has not been presented in the literature.

III EJECTOR CYCLE & GEOMETRY

The Ejector Cycle Refrigeration System (ECRS) examined in this paper is fitted to the 2012-year model Toyota Prius V Hybrid. Figure 1 shows a diagram of the primary components in the Prius V refrigeration system. Figure 1 shows the primary flow of refrigerant from the condenser, and the secondary flow of the refrigerant from the evaporator. These two flow streams are used to construct the entrainment ratio of the ejector. The entrainment ratio is the ratio of the mass flow rate of the secondary fluid to the mass flow rate of the primary fluid

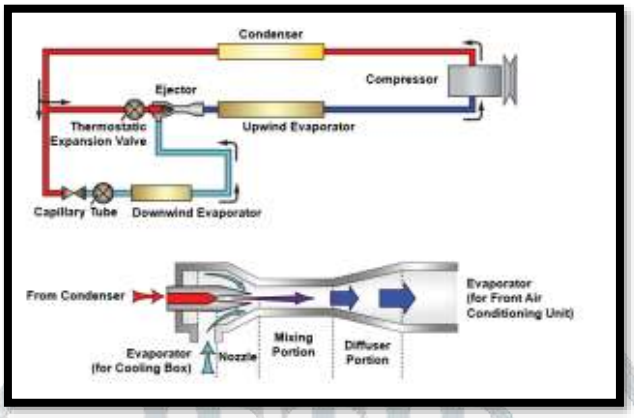

Fig 1 Ejector Refrigeration Cycle

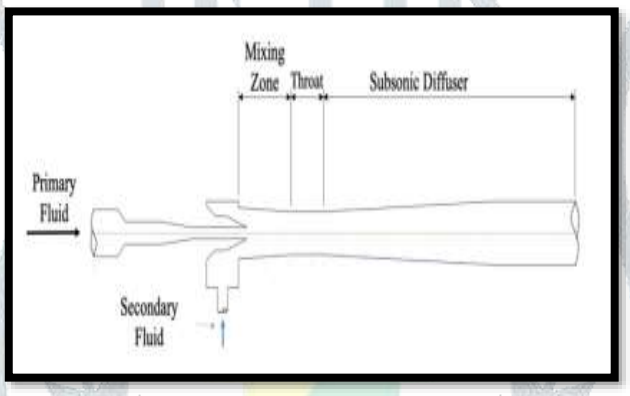

Fig 2 Ejector Geometry

High pressure primary R-1234yf reaches the ejector expands and accelerates through the first nozzle at supersonic speed, creating a low-pressure area. The low-pressure zone and the high-speed R-1234yf draw fluid from the low temperature evaporator through a connecting duct. The secondary 1234yf is cools the primary 1234yf stream. The secondary 1234yf is further accelerated by the high-speed primary 1234yf, until the two mix completely and have a uniform velocity further down the length of the mixing chamber. The now uniform fluid continues down the length of the mixing chamber, where shock diamonds are formed. The end of the diffuser has a higher pressure, which causes backpressure. The shock waves cause compression, and the pressure increases and velocity decreases as the uniform fluid passes through the throat of the ejector. The subsonic diffuser facilitates further pressure rise and velocity drop as the fluid continues down the subsonic diffuser. In the following sections of the paper we present the CFD methodology, model generation, and results of the parametric trade study

IV CFM METHODOLOGY

EJECTOR GEOMETRY

As this analysis uses the DENSO ejector, the geometry of the ejector was re-created from the physical component, which was removed from the 2012 Toyota Prius V. To acquire this hardware, a 2012 Prius V was donated to Citrus College. The HVAC system was removed from the vehicle and the ejector identified.

Measurements were obtained from the physical geometry of the Denso ejector and used to create a 3D model, as shown in Figure. The top panel of Figure shows the full 3D geometry of the ejector, the middle panel of Figure 4 shows a cross-section view of the ejector geometry

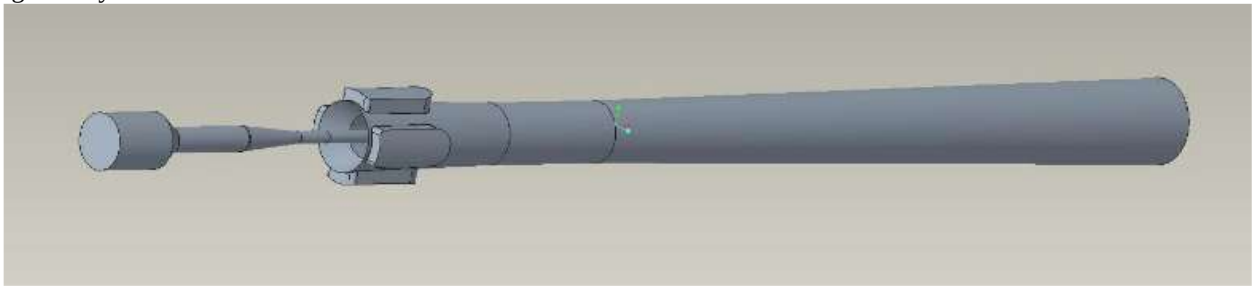

Fig 3 CAD Views of Ejector CAD Model

A 2-D symmetric CAD model was built and imported into ANSYS FLUENT. The energy equation was used, along with the realizable k-ε turbulence model with scalable wall functions. The ejector inlet was specified to be a pressure boundary condition and the suction chamber inlet was given a pressure boundary condition. The outlet was also given a pressure boundary condition. The axisymmetric CFD mesh was created using an all quad-mesh. The mesh used for the simulations is shown in Figure

CFD MESH AND BOUNDARY CONDITIONS

A 2-D symmetric CAD model was built and imported into ANSYS FLUENT. The energy equation was used, along with the realizable k-ε turbulence model with scalable wall functions. The ejector inlet was specified to be a pressure boundary condition and the suction chamber inlet was given a pressure boundary condition. The outlet was also given a pressure boundary condition. The axisymmetric CFD mesh was created using an all quad-mesh. The mesh used for the simulations is shown in Figure

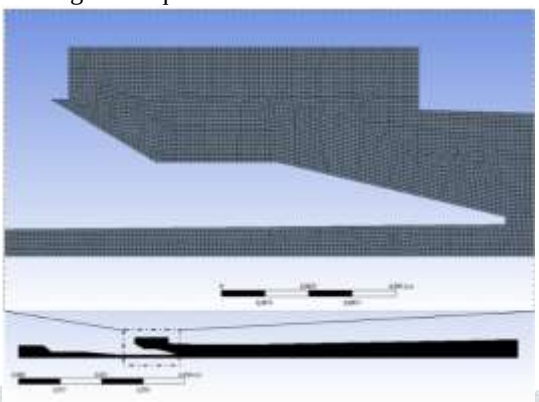

Fig 4 CFD Mesh of Ejector

PARAMETRIC CASES RUN

The performance of the ejector created in the ANSYS FLUENT CFD model was evaluated using three working fluid refrigerants, R-134a, R-1234yf, and R245fa, with the properties shown in figure

Fluid	c_p $\left(\frac{\text{kJ}}{\text{kg}}\right)$	k $\left(\frac{\text{W}}{\text{m}\cdot\text{K}}\right)$	μ $\left(\frac{\text{kg}}{\text{m}\cdot\text{s}}\right)$	MW $\left(\frac{\text{kg}}{\text{kmol}}\right)$
R-134a	0.8435	0.01299	11.62E-6	102.032
R-1234yf	0.8963	0.01322	12.16E-6	114.04
R-245fa	0.8931	0.0125	10.3E-6	134.05

Fig 5 fluid properties

V. RESULTS AND DISCUSSION

In the Baseline evaluation, the ejector inlet pressure, mixing chamber inlet Pressure, and ejector outlet pressures were set to nominal values, as shown in fig . The resulting mass flow rate and entrainment ratio are also shown in Table 2. The baseline simulations show that with the same conditions, the R-245fa working fluid has the highest entrainment ratio, followed by the R-1234yf, and R-134a, respectively.

Fluid	Ejector Inlet Pressure (Pa)	Mixing Chamber Inlet Pressure (Pa)	Ejector Outlet Pressure (Pa)	Mass Flow Rate (kg/s)	Entrainment Ratio,w
R-134a	2.0E5	1.0E5	1.0E5	1.497E-3	2.2729
R-1234yf	2.0E5	1.0E5	1.0E5	1.629E-3	2.4249
R-245fa	2.0E5	1.0E5	1.0E5	1.768E-3	2.4449

Fig 6 Various Mechanical Parameters for Different Refrigerants

The simulation cases varied one of the three pressure boundary conditions, and held the other two constant. The entrainment ratio and mass flow rate were calculated for each of the pressure variation cases. In the first case, the ejector inlet pressure boundary condition was varied from $1.50*10^5$ Pa to $2.50*10^5$ Pa in $0.25*10^5$ Pa increments, with the Mixing Chamber and Outlet Pressures held constant at 1.00´105 Pa. Each respective inlet pressure results in a unique mass flow rate. These mass flow rate values are plotted against the resulting entrainment ratios for each respective working fluid, and are shown in Figure . The dotted lines connecting points across working fluids are lines of constant pressure, showing the pressure that was set to calculate the resulting mass flow rates and entrainment ratios. It is discernable that the R-245fa working fluid has the highest entrainment ratio of =2.4778, at the ejector inlet pressure of $1.75*10^5$ Pa, followed by the R-1234yf and the R-134a, respectively. All three working fluids display a similar behavior in the Inlet Pressure variation cases, the mass flow rates increase as the pressures increase. As pressure increases, the entrainment ratio increases, and then begins to drop after the peak at the pressure of $1.75*10^5$ Pa.

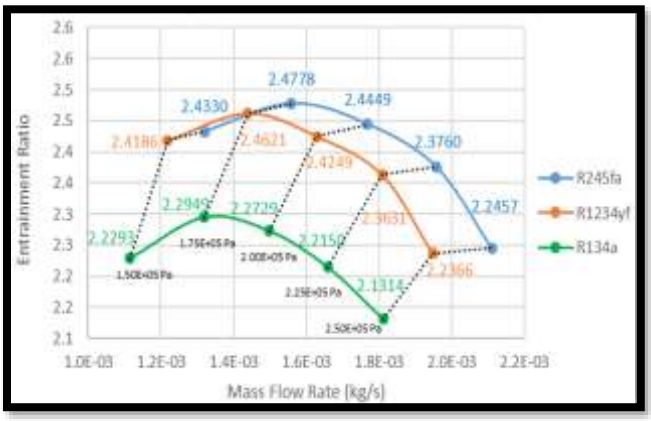

Fig 7 Entrainment Ratio Vs. Mass Flow Rate Case 1

In the second case, the ejector mixing chamber inlet pressure boundary condition was varied from $9.00*10^5$ Pa to $1.10*10^5$ Pa, in a single $2.00*10^4$ Pa interval. The injector inlet pressure was held constant at $2.00*10^4$ Pa, and the injector outlet pressure was held constant at $1.00*10^4$Pa. Figure shows the R245fa working fluid having the highest entrainment ratio of =2.9796, at the ejector mixing chamber inlet pressure of $1.10*10^5$Pa, followed by the R-1234yf and the R-134a, respectively.

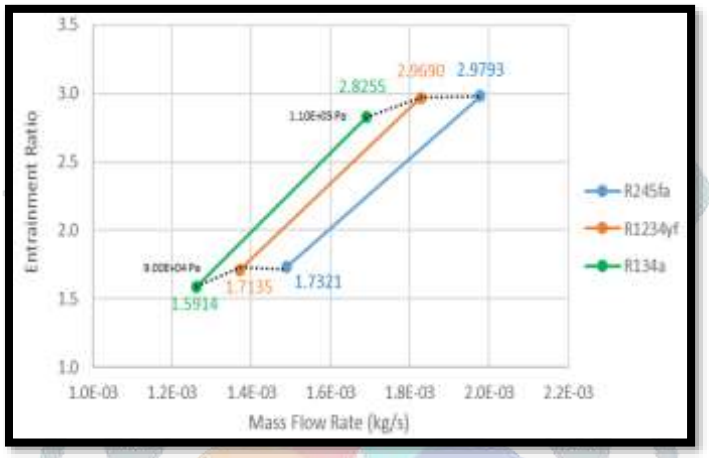

Fig 8 Entrainment Ratio Vs. Mass Flow Rate Plot Case 2

In the third case, the ejector outlet pressure boundary condition was varied from $1.10*10^5$ Pa to $1.20*10^5$ Pa, in a single $0.1*10^5$ Pa interval. The injector inlet pressure was held constant at $2.00*10^5$ Pa and the injector mixing chamber inlet pressure was held constant at $1.00*10^5$ Pa, showing a pressure drop internal to the mixing chamber, with a rise at the exit. Figure shows the R245fa working fluid having the highest entrainment ratio of =1.6813, at the ejector mixing chamber inlet pressure of $1.2*10^5$ Pa, followed by the R-1234yf and the R-134a, respectively.

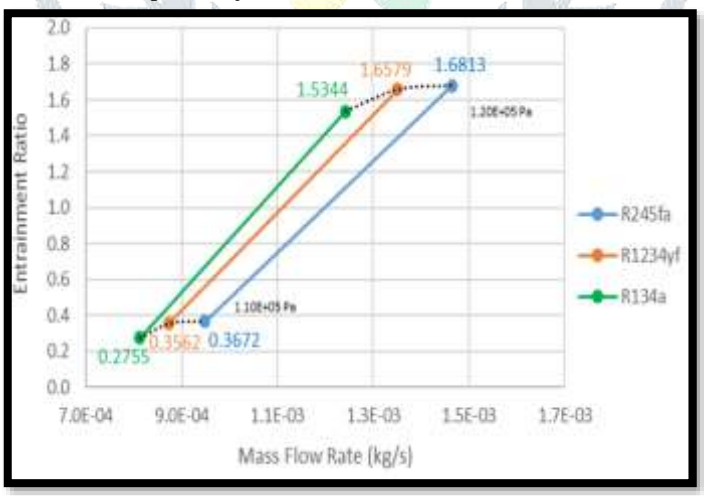

Fig 9 Entrainment Ratio Vs. Mass Flow Rate Plot Case 3

Fig 10 R-134a Pressure Contours

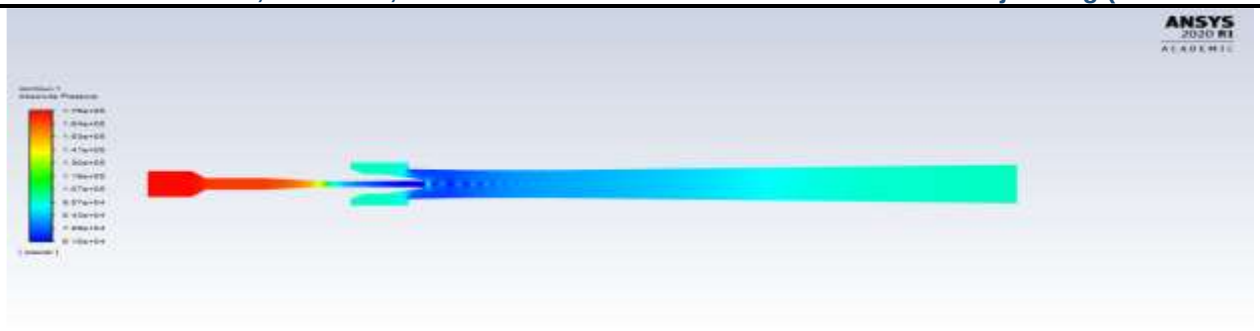

Fig 11 R-245fa Pressure Contours

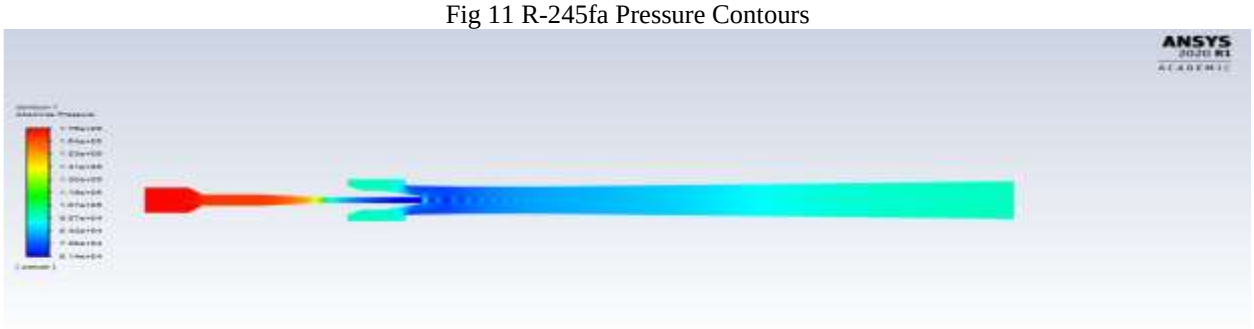

Fig 12 R-1234yf Pressure Contours

The pressure contours of Figures, respectively, show the area of large and small pressures set up in the Venturi section of the ejector. The pressure distribution along the centerline plots of Figures for R-134a, R245fa, and R-1234yf, respectively show the expected distribution of pressure as the flow moves through the ejector, with a high erratic pressure distribution occurring near the throat region of the ejector.

CONCLUSION

This CFD analysis of the DENSO ejector carried out herein shows that R-245fa performs the best out of the three working fluids, when examining their entrainment ratios. In addition, all three working fluid entrainment ratios rose to a peak performance at the ejector inlet pressure of $1.75*10^5$ Pa. The ejector mixing chamber pressure and ejector outlet pressure boundary conditions also saw a rise in entrainment ratios, during an increase of their respective pressure values.

REFERENCES

[1] Honra, Jaime, Menandro S. Berana, Louis Angelo M. Danao, and Mark Christian E. Manuel. "CFD analysis of supersonic ejector in ejector refrigeration system for air conditioning application." In Proceedings of the World Congress on Engineering, London, UK, vol. 2. 2017.

[2] Zheng, Ping, Bing Li, and Jingxuan Qin. "CFD simulation of two-phase ejector performance influenced by different operation conditions." Energy 155 (2018): 1129-1145.

[3] Haida, Michal, Jacek Smolka, Armin Hafner, Ziemowit Ostrowski, Michal Palacz, Andrzej J. Nowak, and Krzysztof Banasiak. "System model derivation of the CO2 two-phase ejector based on the CFD-based reduced-order model." Energy 144 (2018): 941-956.

[4] Wang, Lei, Jia Yan, Chen Wang, and Xianbi Li. "Numerical study on optimization of ejector primary nozzle geometries." International Journal of Refrigeration 76 (2017): 219-229.

[5] Elbarghthi, Anas FA, Saleh Mohamed, Van Vu Nguyen, and Vaclav Dvorak. "CFD Based Design for Ejector Cooling System Using HFOS (1234ze (E) and 1234yf)." Energies 13, no. 6 (2020): 1408.

[6] Van Vu, Nguyen, and Jan Kracik. "CFD simulation of ejector: is it worth to use real gas models?." In EPJ Web of Conferences, vol. 180, p. 02075. EDP Sciences, 2018.

[7] Suvarnakuta, N., K. Pianthong, T. Sriveerakul, and W. Seehanam. "Performance analysis of a two-stage ejector in an ejector refrigeration system using computational fluid dynamics." Engineering Applications of Computational Fluid Mechanics 14, no. 1 (2020): 669-682.

[8] Elhub, B., Sohif Mat, K. Sopian, A. A. Ammar, A. M. Elbreki, and Ammar M. Adulateef. "Computational Fluid Dynamics (CFD) as an Efficient Tool for Ejector Simulations–A Review."

[9] Geng, Lihong, Huadong Liu, and Xinli Wei. "CFD analysis of the flashing flow characteristics of subcritical refrigerant R-134a through converging-diverging nozzles." International Journal of Thermal Sciences 137 (2019): 438-445.